

# Accurate halo-galaxy mocks from automatic bias estimation and particle mesh gravity solvers

Mohammadjavad Vakili<sup>1\*</sup>, Francisco-Shu Kitaura<sup>2,3†</sup>, Yu Feng<sup>4</sup>,  
Gustavo Yepes<sup>5</sup>, Cheng Zhao<sup>6</sup>, Chia-Hsun Chuang<sup>7</sup>, ChangHoon Hahn<sup>1</sup>

<sup>1</sup> *Center for Cosmology and Particle Physics, Department of Physics, New York University, New York, NY, 10003, USA*

<sup>2</sup> *Instituto de Astrofísica de Canarias, 38205 San Cristóbal de La Laguna, Santa Cruz de Tenerife, Spain*

<sup>3</sup> *Departamento de Astrofísica, Universidad de La Laguna (ULL), E-38206 La Laguna, Tenerife, Spain*

<sup>4</sup> *Berkeley Center for Cosmological Physics, Department of Physics, University of California Berkeley, Berkeley CA, 94720, USA*

<sup>5</sup> *Departamento de Física Teórica, Universidad Autónoma de Madrid, Cantoblanco, 28049, Madrid, Spain*

<sup>6</sup> *Tsinghua Center for Astrophysics, Department of Physics, Tsinghua University, Haidian District, Beijing 100084, P. R. China*

<sup>7</sup> *Leibniz-Institut für Astrophysik Potsdam (AIP), An der Sternwarte 16, D-14482 Potsdam, Germany*

August 29, 2017

## ABSTRACT

Reliable extraction of cosmological information from clustering measurements of galaxy surveys requires estimation of the error covariance matrices of observables. The accuracy of covariance matrices is limited by our ability to generate sufficiently large number of independent mock catalogs that can describe the physics of galaxy clustering across a wide range of scales. Furthermore, galaxy mock catalogs are required to study systematics in galaxy surveys and to test analysis tools. In this investigation, we present a fast and accurate approach for generation of mock catalogs for the upcoming galaxy surveys. Our method relies on low-resolution approximate gravity solvers to simulate the large scale dark matter field, which we then populate with halos according to a flexible nonlinear and stochastic bias model. In particular, we extend the PATCHY code with an efficient particle mesh algorithm to simulate the dark matter field (the FASTPM code), and with a robust MCMC method relying on the EMCEE code for constraining the parameters of the bias model. Using the halos in the BigMultiDark high-resolution  $N$ -body simulation as a reference catalog, we demonstrate that our technique can model the bivariate probability distribution function (counts-in-cells), power spectrum, and bispectrum of halos in the reference catalog. Specifically, we show that the new ingredients permit us to reach percentage accuracy in the power spectrum up to  $k \sim 0.4 h \text{ Mpc}^{-1}$  (within 5% up to  $k \sim 0.6 h \text{ Mpc}^{-1}$ ) with accurate bispectra improving previous results based on Lagrangian perturbation theory.

**Key words:** cosmology: observations - distance scale - large-scale structure of Universe

## 1 INTRODUCTION

The current and the next generation of galaxy surveys such as EBOSS<sup>1</sup> (Extended Baryon Oscillation Spectroscopic Survey, Dawson et al. 2016), DESI<sup>2</sup> (Dark Energy Spectroscopic Instrument, Levi et al. 2013), EUCLID<sup>3</sup> (Laureijs et al. 2011), LSST<sup>4</sup> (LSST Science Collaboration et al. 2009), and WFIRST<sup>5</sup> (Spergel et al. 2015)

are expected to achieve unprecedented constraints on the cosmological parameters, growth of structure, expansion history of the universe, and modified theories of gravity. Accurate cosmological inferences with these surveys require accurate computation of the likelihood function of the observed data given a cosmological model. This goal can be achieved provided that the uncertainties, in the form of error covariance matrices in the likelihood functions, are reliably estimated. Therefore, covariance matrices are essential ingredients in extraction of cosmological information from the data.

The most commonly used technique in estimation of the covariance matrix for galaxy clustering observables requires generation of a large number of simulated galaxy mock catalogs. These mock catalogs need to reproduce

\* E-mail: mjvakili@nyu.edu

† E-mail: fkitaura@iac.es

<sup>1</sup> <http://www.sdss.org/surveys/eboss/>

<sup>2</sup> <http://desi.lbl.gov/>

<sup>3</sup> <http://www.euclid-ec.org/>

<sup>4</sup> <http://www.lsst.org/>

<sup>5</sup> <https://www.nasa.gov/wfirst>

the cosmic volume probed by the galaxy surveys. They also need to describe the clustering observables with high accuracy in a wide range of scales. It has been demonstrated that both the precision and the accuracy of constraints on the cosmological parameters, regardless of the details of a given galaxy survey, depend on the number of realizations of the survey (Dodelson & Schneider 2013; Taylor & Joachimi 2014). The requirement on the number of independent realizations of the survey becomes more stringent as the number of data points in a given analysis grows (Taylor et al. 2013). The most pressing challenges ahead of simulating a large number of catalogs are: simulation of large volumes for sampling the Baryonic Acoustic feature in the galaxy clustering, accurate description of the clustering signal at small scales, accurate clustering not only at the level of two-point statistics but also at the level of higher order statistics, and resolving low mass halos that host fainter galaxy samples.

High-resolution  $N$ -body simulations are ideal venues for reproducing the dark matter clustering accurately. But production of a large number of density field realizations with  $N$ -body simulations is not computationally feasible. In order to alleviate the computational cost of  $N$ -body simulations, several methods based on approximate gravity solvers have been introduced. Methods based on higher order Lagrangian perturbation theory (Buchert & Ehlers 1993; Bouchet et al. 1995; Catelan 1995; Monaco et al. 2002; Scoccimarro & Sheth 2002; Kitaura & Heß 2013), Zeldovich approximation (Chuang et al. 2015a), and approximate  $N$ -body simulations (Tassev et al. 2013; White et al. 2014; Howlett et al. 2015; Tassev et al. 2015; Feng et al. 2016; Izard et al. 2016; Koda et al. 2016) have been demonstrated to be promising for fast generation of dark matter density field. Sampling the structures such as galaxies and halos from the dark matter density field requires an additional step. Identification of virialized regions of matter overdensity is either done through a biasing scheme (Kitaura et al. 2014; White et al. 2014) or is done through application of friends-of-friends algorithm (Manera et al. 2013; Koda et al. 2016; Feng et al. 2016). Methods that employ a biasing scheme need to be calibrated such that they are statistically consistent with accurate  $N$ -body simulations or observations.

The PATCHY method (Kitaura et al. 2014, 2015) produces mock catalogs by first generating dark matter field with Lagrangian Perturbation Theory modified with spherical collapse model on small scales ( $r \leq 2 h^{-1}$  Mpc) and then sampling galaxies (halos) from the density field using nonlinear stochastic biasing introduced in Kitaura et al. (2014). This method has been shown to reproduce the two-point clustering with  $\sim 2\%$  accuracy down to  $k \sim 0.3 h \text{ Mpc}^{-1}$  and the counts-in-cells of the massive halos in an accurate  $N$ -body simulation. Kitaura et al. (2015) demonstrate that the mock catalogs generated using this technique are capable of accurately describing the halo bispectrum in the reference  $N$ -body simulations. Furthermore, Kitaura et al. (2016) used this method for massive production of mock catalogs for the cosmological analysis of the completed SDSS III Baryon Oscillation Spectroscopic Survey DR12 galaxy sample.

Alternatively, error covariance matrices can be computed with analytical models (Feldman et al. 1994; Smith et al. 2008; Crocce et al. 2011; Sun et al. 2013; Grieb et al. 2016; Kalus et al. 2016). These methods are promising, though still need further investigation especially including systematic effects, such as the survey geometry. They

will potentially permit us to use a smaller number of mock catalogs to obtain accurate covariance matrices.

In recent years, development of the shrinkage methods (Ledoit & Wolf 2004; Pope & Szapudi 2008; Ledoit & Wolf 2012; Joachimi 2016; Simpson et al. 2016) have been proved promising for alleviating the requirement on the number of mocks. In principle, one could use a combination of the shrinkage methods and a smaller number of mock catalogs to reach the same level of accuracy needed for large scale structure inferences.

Moreover, production of mocks will be a useful tool for investigation of possible sources of systematic errors as well as verification of covariance matrices derived from analytical methods.

In this investigation, we introduce an MCMC method for calibration of the bias model of the PATCHY code. This method constrains the bias parameters by the halo power spectrum and the halo counts-in-cells (halo PDF) of a reference halo catalog constructed from an accurate  $N$ -body simulation.

Furthermore, we replace the dark matter gravity solver of the code with the fast particle-mesh approximate  $N$ -body solver implemented in the FASTPM code (Feng et al. 2016). The advantage of the FASTPM algorithm over other methods based on particle-mesh is its low memory requirements as well as accurate large scale growth. In addition, the dark matter density field produced by the FASTPM code yields better nonlinear clustering than that of the perturbation theory.

As a proof of concept, we make use of the halos in the BigMultiDark Planck high-resolution  $N$ -body simulation (Klypin et al. 2016). This catalog has been extensively used for validation, comparison and production of galaxy mock catalogs (Chuang et al. 2015b; Zhao et al. 2015; Kitaura et al. 2016; Rodríguez-Torres et al. 2016). In addition, we will make a statistical comparison between our PATCHY mocks and the reference catalog. We present the number density, halo PDF (halo counts-in-cells), and halo two-point statistics. We also present our results in terms of the three-point statistics since it is rising as a major complementary approach in various large-scale structure analyses (Slepian et al. 2015; Gil-Marín et al. 2015a,b; Guo et al. 2016; Slepian et al. 2016a,b; Gil-Marín et al. 2017).

The remainder of this paper is structured as follows: In section §2, we present our method for generating and calibrating mock catalogs. This includes description of the structure formation model, nonlinear stochastic bias model of the PATCHY code, and our MCMC method for constraining the bias parameters. In section §3, we describe how different pieces of code are integrated into the PATCHY method. We illustrate the performances using a reference halo catalog constructed from an accurate  $N$ -body simulation in section §4, and we discuss the main results and present our conclusions in section §5.

## 2 METHODOLOGY

Our method consists of producing the large scale dark matter field on a mesh and then populating it with halos (or galaxies) with a given bias model. The parameters of that bias model are constrained with a reference catalog in an automatic statistical way. Our approach is agnostic about the method used for identification of halos in the reference catalog. The PATCHY code permits us to sample

galaxies directly from the density field. For instance [Kitaura et al. \(2016\)](#) samples mock galaxy catalogs based on an accurate reference mock galaxy catalog ([Rodríguez-Torres et al. 2016](#)). Let us first describe in §2.1 the new implementation of the structure formation in PATCHY, followed in §2.2 by the bias model, and finally in §2.3 our novel MCMC sampling procedure to obtain the bias parameters.

## 2.1 Structure formation model

Originally, the PATCHY code used Augmented Lagrangian Perturbation Theory (ALPT, [Kitaura & Heß 2013](#)) as a structure formation model. In this model the second order Lagrangian perturbation theory is modified by employing a spherical collapse model on small comoving scales ( $r \leq 2 h^{-1} \text{Mpc}$ ). Any LPT based approximation will lack the one halo term in the clustering. This can be partially compensated within the bias model, however, at the price of obtaining a less accurate description of the biasing relation. Therefore we introduce in this work within the PATCHY code the fast particle mesh code FASTPM ([Feng et al. 2016](#)). In FASTPM, the kick and drift steps of the PM codes are modified such that the linear growth of structure is exact. [Feng et al. \(2016\)](#) demonstrates that the memory requirements of this algorithm are much lower than those of the COmoving Lagrangian Acceleration  $N$ -body solver (COLA, [Tassev et al. 2013](#)).

Moreover, [Feng et al. \(2016\)](#) shows that running the code with relatively few time steps, and applying a friends-of-friend (hereafter fof) halo finder ([Davis et al. 1985](#)) to the density field, one can accurately recover the redshift space power spectrum of the fof halos of TreePM accurate  $N$ -body solver ([Bagla 2002](#)) down to  $k \sim 0.5 h \text{Mpc}^{-1}$ . The linking length of 0.2 was chosen to be consistent with other works in the literature ([Tassev et al. 2013](#)). In this work we run the FASTPM code with 10 time steps.

In  $N$ -body simulations, the dark matter density field is evolved by solving the Boltzmann and Poisson equations in an expanding background. Particle Mesh (PM) gravity solvers are a class of  $N$ -body solvers in which the evolution of the density field is governed by the dynamic of dark matter particles. These dark matter particles are evolved with a finite number of time steps.

Furthermore, in PM solvers, the density field is realized on a mesh with an interpolation scheme (for example CIC) that assigns particles to grid points. Then the gravitational Potential (and subsequently the gravitational force) is estimated by solving the Poisson equation. This grid-based estimation of gravitational forces results in compensation of accuracy on scales comparable to the spacing between grid points. In TREEPM algorithm on the contrary, small-scale force calculation can be fully resolved by direct summation of pairs with a spacing comparable to the spacing between grid points. By growth of the matter overdensity however, the computing time required for the direct summation scheme quickly increases.

The time steps in a PM simulation are either linearly or logarithmically spaced in scale factor. Logarithmic spacing of time steps have the disadvantage of losing accuracy in terms of small-scale power and halo mass function. On the other hand, choosing time steps that are linear in scale factor leads to more accurate clustering on small scales. It is important to note that finite number of

time steps in PM simulations results in inaccurate large-scale growth.

In FastPM, corrections are applied to the equations of motions of particles such that exact large-scale growth is imposed. In particular, the error in large scale growth is corrected by using the Zeldovic equations of motion to modify the kick and drift operations in a pure PM algorithm. In a PM simulation, the drift operator changes the position of each particle by keeping its momentum fixed. On the other hand, the kick operator changes the momentum of each particle while leaving its position unchanged. The modified Kick and Drift operators of FastPM are derived by integration of the Zeldovic Approximation equations of motion. As a result, exact large scale growth is imposed in FastPM and in the limit of infinitesimal time steps the Kick and Drift operators of FastPM converge to those of a standard PM algorithm.

In this work we will use as a reference the high-resolution  $N$ -body BigMultiDark simulation described in more detail in section §4.1. A comparison of the dark matter density fields obtained with the different methods is shown in Fig. 1. While the structures in the high-resolution  $N$ -body simulation and the low-resolution FASTPM simulation look very similar in spite of having very different resolutions ( $3840^3$  vs  $960^3$  particles), the low-resolution ALPT simulation looks more diffuse due to the exaggerated shell crossing inherent to LPT based methods. We will study the impact of this inaccuracy in more detail in section §4.3.

## 2.2 Sampling halos from the density field

In this section, we describe the statistical bias model of the PATCHY code. This model generates halos/galaxies from a given dark matter density field and consists of: deterministic bias, stochastic bias, and an additional step for applying redshift space distortions (RSDs) to the catalogs. We describe the bias steps below and leave RSDs for a later work.

### 2.2.1 Deterministic bias

The expected number of halos  $\langle \rho_h \rangle$  in a given volume element  $dV$  (cosmic cell) can be described in general by a deterministic bias relation  $B(\rho_h|\rho_m)$ :

$$\langle \rho_h \rangle_{dV} = f_h B(\rho_h|\rho_m), \quad (1)$$

where  $\rho_m$  is the matter density field. The prefactor  $f_h$  is an overall normalization factor which can be determined by requiring the halo density field to have the number density of the reference sample  $n_h$ , i.e.,  $n_h = \langle \langle \rho_h \rangle_{dV} \rangle_V$ . Formally, this can be written as

$$f_h = \frac{n_h}{\langle B(\rho_h|\rho_m) \rangle_V}, \quad (2)$$

where  $\langle \cdot \rangle_V$  is an ensemble volume average. In particular, we will adopt the following compact deterministic bias model:

$$B(\rho_h|\rho_m) = \underbrace{\rho_m^\alpha}_{\text{nonlinear bias}} \times \underbrace{\theta(\rho_m - \rho_{th})}_{\text{threshold bias}} \times \underbrace{\exp(-(\rho_m/\rho_\epsilon)^\epsilon)}_{\text{exponential cutoff}}, \quad (3)$$

where  $\rho_{th}$  is the density threshold which suppresses halo formation in under-dense regions, and  $\alpha$  is a nonlinear

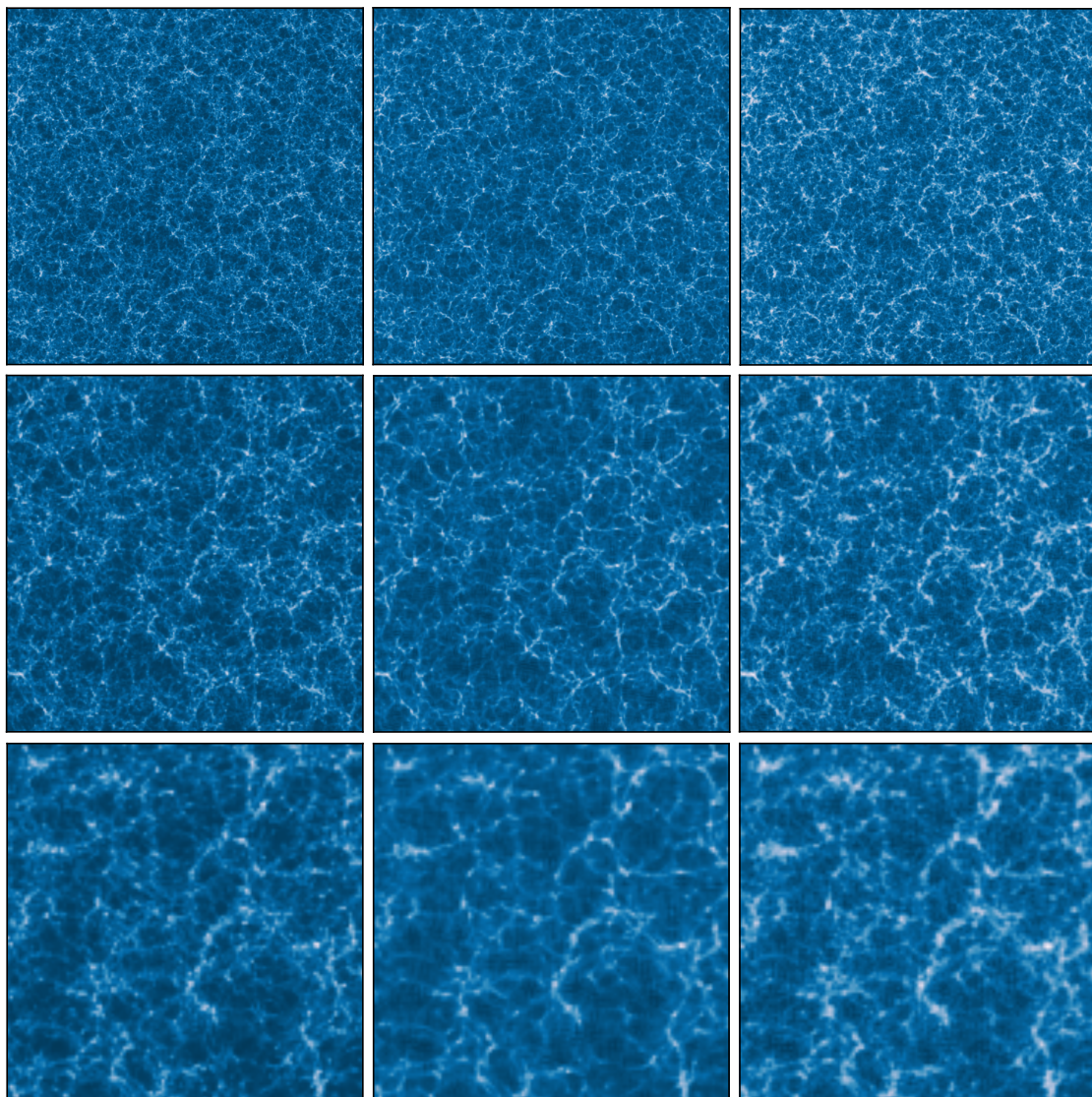


**Figure 1.** Dark matter overdensity  $\delta = \rho_m/\rho - 1$  slices of  $20 h^{-1} \text{Mpc}$  from the high-resolution BigMultiDark simulation (left panels), the low-resolution FASTPM simulation (central panels) and from the ALPT simulation (right panels), taking a subvolume of  $(1250 h^{-1} \text{Mpc})^3$  (top panels),  $(625 h^{-1} \text{Mpc})^3$  (middle panels), and  $(312.5 h^{-1} \text{Mpc})^3$  (bottom panels). The structures in the high-resolution  $N$ -body simulation and the low-resolution FASTPM simulation look very similar in spite of having very different resolutions ( $3840^3$  vs  $960^3$  particles). The low-resolution ALPT simulation with a resolution of  $960^3$  looks more diffuse.

bias parameter. The threshold bias (Kaiser 1984; Bardeen et al. 1986; Sheth et al. 2001; Mo & White 2002) is modeled by a step function  $\theta(\rho_m - \rho_{\text{th}})$  (Kitaura et al. 2014) and an exponential cutoff  $\exp(-(\rho/\rho_\epsilon)^\epsilon)$  (Neyrinck et al. 2014). Therefore, for this particular bias model we have a normalization of

$$f_{\text{h}} = \frac{n_{\text{h}}}{\langle \theta(\rho_m - \rho_{\text{th}}) \rho_{\text{m}}^\alpha \exp(-(\rho_m/\rho_\epsilon)^\epsilon) \rangle_V}. \quad (4)$$

The advantage of this kind of bias model is that it is flexible and it is able to incorporate additional terms and each of the terms has a physical interpretation. The power law bias stands for one of the simplest possible non-linear bias models: a linear Lagrangian bias in a comoving framework, which can be derived from the lognormal approximation (see Kitaura et al. 2014), and it resumes in one single bias parameter an infinite Taylor expansion of the dark matter density field (Cen & Ostriker 1993; Fry & Gaztanaga 1993; de la Torre & Peacock 2013).

The threshold bias and the exponential cut-off describe the fact that halos (or galaxies) can only reside in

regions which contain a minimum mass. They also represent the loss of information with respect to the full cosmic density field from selecting only gravitationally collapsed objects.

### 2.2.2 Stochastic bias

The number of halos in each cell is drawn from a Negative Binomial (NB) distribution which can be characterized by the expected number of halos in the cell  $\lambda_{\text{h}} = \langle \rho_{\text{h}} \rangle_{\text{dV}} \times \text{dV}$ , and a parameter  $\beta$  which quantifies the stochasticity (deviation of the distribution from Poissonity) in the halo distribution. According to this model, the probability of

having  $N_h$  objects in a volume element is given by

$$P(N_h|\lambda_h, \beta) = \underbrace{\frac{\lambda_h^{N_h}}{N_h!} e^{-\lambda_h}}_{\text{Poisson distribution}} \times \underbrace{\frac{\Gamma(\beta + N_h)}{\Gamma(\beta)(\beta + \lambda_h)^{N_h}} \times \frac{e^{\lambda_h}}{(1 + \lambda_h/\beta)^\beta}}_{\text{Deviation from Poissonity}}. \quad (5)$$

For  $\beta \rightarrow \infty$  we can show that the second row in the above equation goes to one. Since  $\Gamma(\beta) = \frac{\Gamma(\beta+1)}{\beta} = \frac{\Gamma(\beta+N_h)}{\beta(\beta+1)\dots(\beta+N_h-1)}$ , the first factor can be written as  $\frac{\Gamma(\beta+N_h)}{\Gamma(\beta)(\beta+\lambda_h)^{N_h}} = \frac{\beta(\beta+1)\dots(\beta+N_h-1)}{(\beta+\lambda_h)^{N_h}} = \frac{(1+1/\beta)\dots(1+(N_h-1)/\beta)}{(1+\lambda_h/\beta)^{N_h}}$ . It is now straightforward to see that this goes to one for  $\beta \rightarrow \infty$ . The same happens for the second factor  $\frac{e^{\lambda_h}}{(1+\lambda_h/\beta)^\beta} \rightarrow 1$ , since  $(1+\lambda_h/\beta)^\beta \rightarrow e^{\lambda_h}$  in that limit.

Given a dark matter density field  $\rho_m$ , the halo density field can be constructed by drawing samples from the expected halo density field  $\rho_h$  with the Negative-Binomial (hereafter NB) distribution (Eq. 5). This is inspired by the fact that the excess probability of finding halos in high density regions generates over-dispersion (Somerville et al. 2001; Casas-Miranda et al. 2002). This over-dispersion is modeled by a NB distribution (Kitaura et al. 2014; Neyrinck et al. 2014).

The stochastic bias stands for the shot noise from the transition of the continuous dark matter field to the discrete halo (or galaxy) distribution. As predicted by Peebles (1980), it produces a dispersion larger than Poisson, as long as the two-point correlation function remains positive below the scale of the cell size. This is captured by the negative binomial PDF (Eq. 5).

### 2.3 Constraining the bias model

Production of approximate mock catalogs with PATCHY requires a reference catalog constructed from the observations or based on an accurate  $N$ -body simulation. We aim at constraining the parameters describing the deterministic bias  $\{\delta_{\text{th}}, \alpha, \rho_\epsilon, \epsilon\}$ , and the parameter that governs the stochasticity of the halo population  $\{\beta\}$ .

The bias parameters are estimated such that the statistical summaries of the halos (galaxies) in the PATCHY mocks match the statistical summaries of the halos (galaxies) in the reference catalog. The set of statistical summaries of the catalog can in principle include number density, bivariate probability distribution function or number of counts-in-cells  $\rho(\cdot)$ , two-point statistics  $\xi_2$ , and higher-order statistics such as the three-point statistics  $\xi_3$ . Note that the number of counts-in-cells is defined as the number of cells that contain a given number of halos.

By construction, the PATCHY mocks reproduce the exact number density of objects in the reference catalog. This comes from the particular choice of normalization in the deterministic bias relation (see Eqs. 3,4). In this work, we follow Kitaura et al. (2015) and constrain the bias parameters with the halo PDF and the two-point statistics  $\xi_2$ . These two quantities can be computed very fast and the skewness of the halo PDF determines the three point statistics. Given the bias parameters found by fitting the PDF and the two-point statistics, we will demonstrate a comparison between the approximate mocks and the reference catalog in terms of the two- and three-point statistics.

We simultaneously fit the real-space power spectrum  $P(k)$  and the PDF  $\rho(n)$  of the PATCHY halo density field to  $P(k)$  and  $\rho(n)$  measured for the BigMultiDark halo catalog. Specifically, constraints on  $\theta = \{\delta_{\text{th}}, \alpha, \rho_\epsilon, \epsilon, \beta\}$  are found by sampling from the posterior probability  $p(\theta|\text{data}) \propto p(\text{ref}|\theta)p(\theta)$ , where ref denotes the combination  $\{P_{\text{ref}}(k), \rho_{\text{ref}}(n)\}$ , and the likelihood  $p(\text{ref}|\theta)$  is given by

$$p(\text{ref}|\theta) = p(P_{\text{ref}}(k)|\theta)p(\rho_{\text{ref}}(n)|\theta), \quad (6)$$

where Gaussian likelihoods are assumed for  $P_{\text{ref}}(k)$  and  $\rho_{\text{ref}}(n)$ :

$$p(P_{\text{ref}}(k)|\theta) = \prod_k \frac{1}{\sqrt{2\pi\sigma_k^2}} \times \exp\left[-\frac{(P_{\text{ref}}(k) - P_{\text{mock}}(k))^2}{2\sigma_k^2}\right], \quad (7)$$

$$p(\rho_{\text{ref}}(n)|\theta) = \prod_n \frac{1}{\sqrt{2\pi\sigma_n^2}} \times \exp\left[-\frac{(\rho_{\text{ref}}(n) - \rho_{\text{mock}}(n))^2}{2\sigma_n^2}\right]. \quad (8)$$

As a result:

$$-2 \ln p(\text{ref}|\theta) = \sum_k \left[ \frac{(P_{\text{ref}}(k) - P_{\text{mock}}(k))^2}{\sigma_k^2} + \ln(2\pi\sigma_k^2) \right] + \sum_n \left[ \frac{(\rho_{\text{ref}}(n) - \rho_{\text{mock}}(n))^2}{\sigma_n^2} + \ln(2\pi\sigma_n^2) \right] \quad (9)$$

For the purpose of estimating the bias parameters, we find it sufficient to assume simple uncorrelated noise terms  $\{\sigma_k, \sigma_n\}$  in the above likelihood (9). We assume  $\sigma_k^2$  to be  $4\pi^2 P_{\text{ref}}^2(k)/(V_{\text{box}} k^2 \Delta k)$ , and  $\sigma_n^2$  to be  $N_n$  where  $N_n$  is the number of cells containing  $n$  number of halos (including parent halos and subhalos).

In Eq. 9, a Gaussian likelihood is assumed. It is worth noting that the relative weight between the two terms in the likelihood function is determined by their corresponding bin sizes. For instance, increasing the size of the  $n$ th bin in the term corresponding to the PDF in Eq. 9, will increase  $N_n$  and as a result  $\sigma_n$ . This gives more weight to the power spectrum and reduces the prediction power of the halo PDF. We find that giving more weight to the power spectrum results in higher deviations from Poissonity (higher stochasticity). Higher stochasticity (lower  $\beta$ ) leads to enhancement of small-scale power but at the cost of reducing the quality of fit for the halo PDF. This leads to less accurate bispectrum.

Furthermore, we choose a flat prior for all parameters of the bias model with the following lower and upper bounds:  $-1 < \delta_{\text{th}} < 2$ ,  $0 < \alpha < 1$ ,  $0 < \beta < 1$ ,  $0 < \rho_\epsilon < 1$ , and  $0 < \epsilon < 1$ .

For sampling from the posterior probability, given the likelihood function (Eq. 9) and the prior, we use the affine-invariant ensemble MCMC sampler (Goodman & Weare 2010) and its implementation EMCEE (Foreman-Mackey et al. 2013). In particular, we run the EMCEE code with 10 walkers and we run the chains for at least 2000 iterations. We discard the first 500 chains as burn-in samples and use the remainder of the chains as production MCMC chains. Furthermore, we perform Gelman-Rubin

convergence test (Gelman & Rubin 1992) to ensure that the MCMC chains have reached convergence.

## 2.4 Comparison with other approximate methods

Pioneering fast halo/galaxy generating methods have relied on approximate gravity solvers based on Lagrangian perturbation theory (LPT: Buchert & Ehlers 1993; Bouchet et al. 1995; Catelan 1995; Scoccimarro & Sheth 2002) to compute the positions and masses of the objects, such as PINOCCHIO (Zeldovich: Monaco et al. 2002, 2013, 3LPT: Monaco 2016), and PTHALOS (2LPT: Manera et al. 2013, 2015).

This has the disadvantage of being affected by an inaccurate description of the small scale clustering, and, in particular, of missing the one halo term contribution. As a consequence, the power spectra of such catalogs have systematic deviations towards high values of  $k$ , already deviating about 10% at  $k \sim 0.2 h \text{ Mpc}^{-1}$  (Monaco et al. 2013).

While fast particle mesh solvers, such as COLA or FASTPM, are much more precise than LPT based approaches, they are still computationally too expensive to be suitable for massive production, if one is trying to resolve all the necessary structures required to model next generation of galaxy surveys.

Therefore four methods were recently proposed: PATCHY (Kitaura et al. 2014), QPM (White et al. 2014), EZMOCKS (Chuang et al. 2015a), and HALOGEN (Avila et al. 2015), which do not try to resolve halos (nor galaxies) with the approximate gravity solvers, but just get a reliable large scale dark matter field, which can then be populated with some bias prescription. The gravity solver thus only needs to be accurate on a certain scale, then the halo/galaxy-dark matter connection is exploited to reach a high accuracy, as described above.

These methods use both different gravity solvers and different bias models. While PATCHY originally relies on ALPT, QPM uses a quick particle mesh solver, EZMOCKS uses the Zeldovich linear LPT, and HALOGEN uses 2LPT. But more importantly the bias prescriptions follow very different philosophies. QPM uses a rank ordering scheme relating the halo mass to density peaks. Large scale halo bias and halo mass function are recovered in this algorithm. Similarly, HALOGEN relies on first, sampling a number of halo masses from a mass function in discrete mass bins. Then in each mass bin (rank-ordered from high mass to low mass), halos are assigned to cosmic cells according to a distribution function governed by a parameter. This parameter is determined by fitting the two-point function of halos in that mass bin to that of an accurate reference  $N$ -body catalog. Therefore, this algorithm is designed to recover the mass-dependent halo bias of a target  $N$ -body simulation. However, a recent study demonstrated that the dependence of the halo mass to its environment is not trivial (see Zhao et al. 2015). EZMOCKS, on the other hand, first modifies the initial power spectrum introducing a tilt to adjust the final two point statistics, correcting hereby the missing one halo term of the approximate gravity solver. Second it imposes the halo PDF, which was shown to determine the 3pt statistics (Kitaura et al. 2015).

PATCHY on the other hand follows a more physical approach, relying on an effective analytical stochastic bias model. In this sense the statistics is not directly imposed

as in EZMOCKS, but fitted through the bias parameters. In fact PATCHY was shown to be considerably more accurate than EZMOCKS when assigning halo masses (Zhao et al. 2015), and than QPM when fitting the two and three point statistics of the luminous red galaxies (LRGs) in the Baryon Oscillation Spectroscopic Survey (BOSS) (Kitaura et al. 2016).

Relying only on particle mesh gravity solvers for production of mock catalogs is more computationally demanding. That is, in order to resolve all structures (and substructures) one needs to run a PM code with a higher resolution than what is required by PATCHY. For instance Chuang et al. (2015b) found that in order to reproduce distinct (parent) halos of the BigMultiDark simulation, COLA needs a particle-mesh size of  $1280^3$ . This is far away from reproducing the substructures (subhalos). PATCHY on the other hand, requires a smaller grid size of  $960^3$  for production of distinct (parent) halos and subhalos (see Chuang et al. 2015b). In this work we use a grid size of  $960^3$  for generation of both ALPT and FASTPM density fields.

Furthermore, the findings of Feng et al. (2016) suggest that in order to recover the halo mass function of an accurate  $N$ -body simulation with a PM solver and a friends-of-friends halo finding algorithm, one needs to choose a force resolution (the ratio of the grid size and the number of particles on one side of a PM simulation) greater than or equal to two. That is, the mass resolution of a PM simulation for which the grid size and the number of particles are equal, is not sufficient to resolve distinct halos. On the other hand, using simulations with low mass resolution and stochastic biasing methods such as PATCHY and QPM can accurately recover the clustering statistics of halos and subhalos in accurate  $N$ -body simulations.

Moreover, the approach we follow in PATCHY tests the validity range of effective bias prescriptions commonly used in large scale structure analysis methods (see e.g. Ata et al. 2015). Now for the first time we include a robust MCMC sampling scheme to determine the bias parameters, and have improved the gravity solver with FASTPM.

## 3 CODE INTEGRATION

In this section, we briefly explain how different pieces of the PATCHY code are connected. The first step is specification of the cosmological parameters and the initial matter power spectrum. Afterwards, the initial conditions can be provided to the FASTPM code in the form of a white noise (compatible with the initial power spectrum), or they can be randomly drawn from the power spectrum in the FASTPM code.

Once the dark matter particles are evolved with the particle-mesh code until the final redshift, the positions of particles are recorded with the FASTPM code. Then within the PATCHY code, the final particle positions are painted onto a mesh with Cloud-in-Cell (CIC) algorithm. A set of PATCHY bias parameters and the density mesh are the main ingredients for generating a catalog of tracers (galaxies/halos) of the dark matter density field.

The bias parameters are estimated by MCMC in the following way: In an MCMC wrapper, the posterior probability distribution is defined as a function of PATCHY bias parameters. We use the EMCEE code to sample from this posterior probability distribution in the wrapper. For

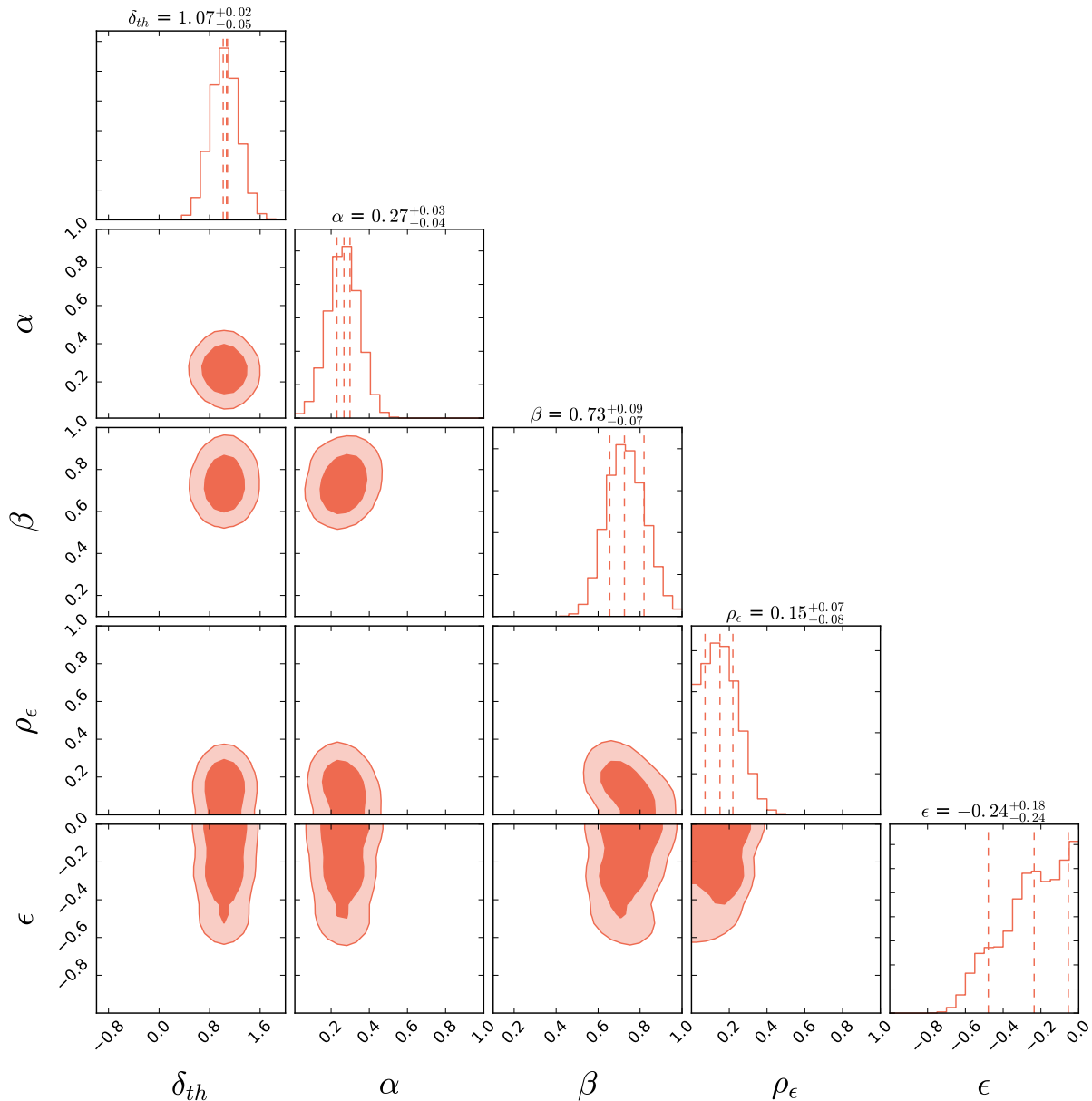


**Figure 2.** Posterior probability distribution of the PATCHY bias parameters  $\{\delta_{th}, \alpha, \beta, \rho_\epsilon, \epsilon\}$ . The contours mark the 68% and the 95% confidence intervals of the posterior probabilities. The vertical lines represent the best estimate and the error bars corresponding to the 50% and 68% confidence intervals obtained from the marginalized posterior distribution over PATCHY bias parameters. This plot is made using the open-source software CORNER (Foreman-Mackey 2016).

each set of bias parameters, a catalog of galaxies/halos is generated from the density mesh with the PATCHY code. Once a catalog is generated, the PDF and the real-space power spectrum of halos in the mock catalogs are evaluated for computation of the likelihood (9).

#### 4 DEMONSTRATION ON AN ACCURATE N-BODY BASED HALO CATALOG

In this section we present the application of the above described method to a well studied case: the halo distribution required to describe the CMASS LRG sample of the BOSS survey (White et al. 2011; Dawson et al. 2013). First, we briefly describe the reference catalog and then present a detailed statistical analysis of the results.

#### 4.1 Reference catalog

For the reference simulation used in this work we rely on the Bound-Density-Maxima (BDM, Klypin & Holtzman 1997) halo catalogs in the  $z = 0.5618$  snapshot of the BigMultiDark-Planck high resolution  $N$ -body simulation (Klypin et al. 2016). This simulation was carried out using the L-Gadget2 code (Springel 2005), following the Planck  $\Lambda$ CDM cosmological parameters  $\Omega_m = 0.307$ ,  $\Omega_b = 0.048$ ,  $\Omega_\Lambda = 0.693$ ,  $\sigma_8 = 0.823$ ,  $n_s = 0.96$ ,  $h = 0.678$ . The box size for this  $N$ -body simulation is  $2500 h^{-1}$  Mpc, the number of simulation particles is  $3840^3$ , the mass per simulation particle  $m_p$  is  $2.359 \times 10^{10} h^{-1} M_\odot$ , and the gravitational softening length  $\epsilon$  is  $30 h^{-1}$  kpc at high- $z$  and  $10 h^{-1}$  kpc at low- $z$ .

A minimum mass cut of  $0.5 \times 10^{13} h^{-1} M_\odot$  has been applied to the halo catalog so that it matches with the number density of the SDSS III-BOSS CMASS galaxy

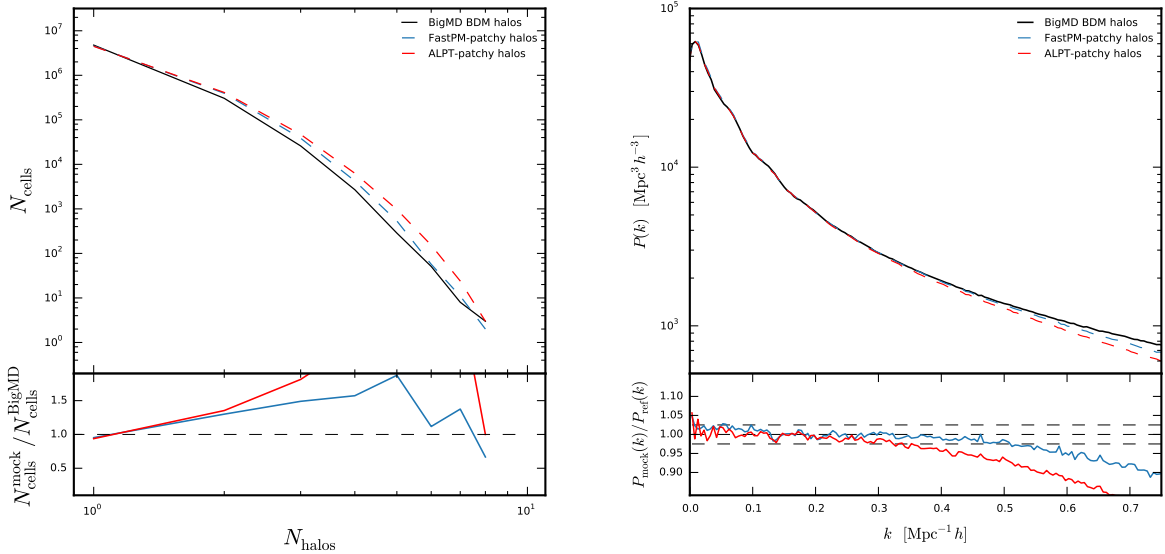


**Figure 3.** Top: Demonstration of the halo bivariate probability distribution function of halos (halo counts-in-cells) in the BigMultiDark simulation (shown in black) and in the FASTPM-PATCHY simulation (shown in blue) and in the ALPT-PATCHY simulation (shown in red) on the left. Comparison between the real-space power spectrum of the BDM halos (shown in black) in the reference BigMultiDark simulation and that of the halos in the FASTPM-PATCHY (ALPT-PATCHY) simulation shown in blue (red) on the right. Bottom: Ratio between the halo PDFs of the approximate mocks and halo PDF of the BigMultiDark simulation on the left. Ratio between the halo power spectra of the approximate mocks and the halo power spectrum of the BigMultiDark simulation on the right.

catalog (White et al. 2011; Dawson et al. 2013). After applying the mass cut, the number density of the final catalog is  $3.5 \times 10^{-4} (h \text{ Mpc}^{-1})^3$ . The MultiDark-PATCHY galaxy catalogs (Kitaura et al. 2016) are calibrated against BOSS-HAM catalogs which were constructed by populating the halos in different snapshots of the BigMultiDark simulation using halo abundance matching (Rodríguez-Torres et al. 2016).

Evaluation of  $P(k)$  and  $\rho(n)$  for a set of bias parameters requires running the forward model of generating halos from the matter density field. Therefore, in order to speed up the fitting procedure we run the PATCHY code with a smaller box size of  $625 h^{-1} \text{ Mpc}$  and grid size of 240 in each dimension. This choice of box and grid size preserves the resolution. Furthermore, running the PATCHY code and computing the statistics of the halo catalogs in a smaller box size significantly reduces the computational time needed for constraining the bias parameters.

## 4.2 Bias parameters

The first step in our pipeline consists of producing the large scale dark matter field on a mesh. We use the down-sampled white noise of the BigMultiDark simulation from  $3840^3$  to  $960^3$  cells to estimate the initial conditions used for both FASTPM and ALPT runs, as shown in Fig. 1. The dark matter particles are then assigned to a mesh of  $960^3$  cells with clouds-in-cells (CIC), which we define as the large scale dark matter density field  $\rho_m$  required for Eqs. 3, 4, 5.

After running the MCMC chains with the method described in section §2, we find constraints on the bias parameters of such equations. These constraints are summarized in Fig. 2. The threshold bias parameter  $\delta_{\text{th}}$  is found to be 1.07 which is equivalent to sampling halos

from the regions of high matter overdensity. This supports our intuition that massive halos are generated from high density regions. Our estimated value of the nonlinear bias parameter  $\alpha$  is  $\sim 0.2$ . These values are qualitatively consistent with ALPT (Kitaura et al. 2014), although the threshold bias is slightly reduced and the power law bias is slightly higher (parameters with ALPT:  $\delta_{\text{th}} \sim 1.2$  and  $\alpha \sim 0.12$ ).

The parameter that governs the deviation from Poissonity  $\beta$  is found to be 0.73. This value is significantly larger than the one found with ALPT (about 0.6), i.e., indicating that the deviation from Poissonity is not so pronounced, as previously found. The reason for this, is that Lagrangian perturbation theory does not manage to model the one halo term, as done with FASTPM. Therefore a larger deviation of Poissonity had to be assumed to fit the power spectrum towards small scales, as is demonstrated here. In this sense, a more accurate description of the large scale dark matter field permits us to reduce the stochasticity in the halo distribution.

Furthermore, parameters corresponding to the exponential cutoff term in the deterministic bias relation  $\{\rho_\epsilon, \epsilon\}$  are estimated to be  $\sim \{0.15, -0.24\}$ . While the constraints on both parameters of the exponential cutoff bias are consistent with zero, their presence, albeit being small, is essential in a more accurate modeling of the halo bivariate PDF and the halo bispectrum. By including these extra parameters we demonstrate the flexibility and efficiency of the code to incorporate complex bias models. Furthermore, we believe that the exponential cutoff term will become crucial when considering smaller mass halos, which have a non negligible probability of residing in low density regions (Neyrinck et al. 2014).



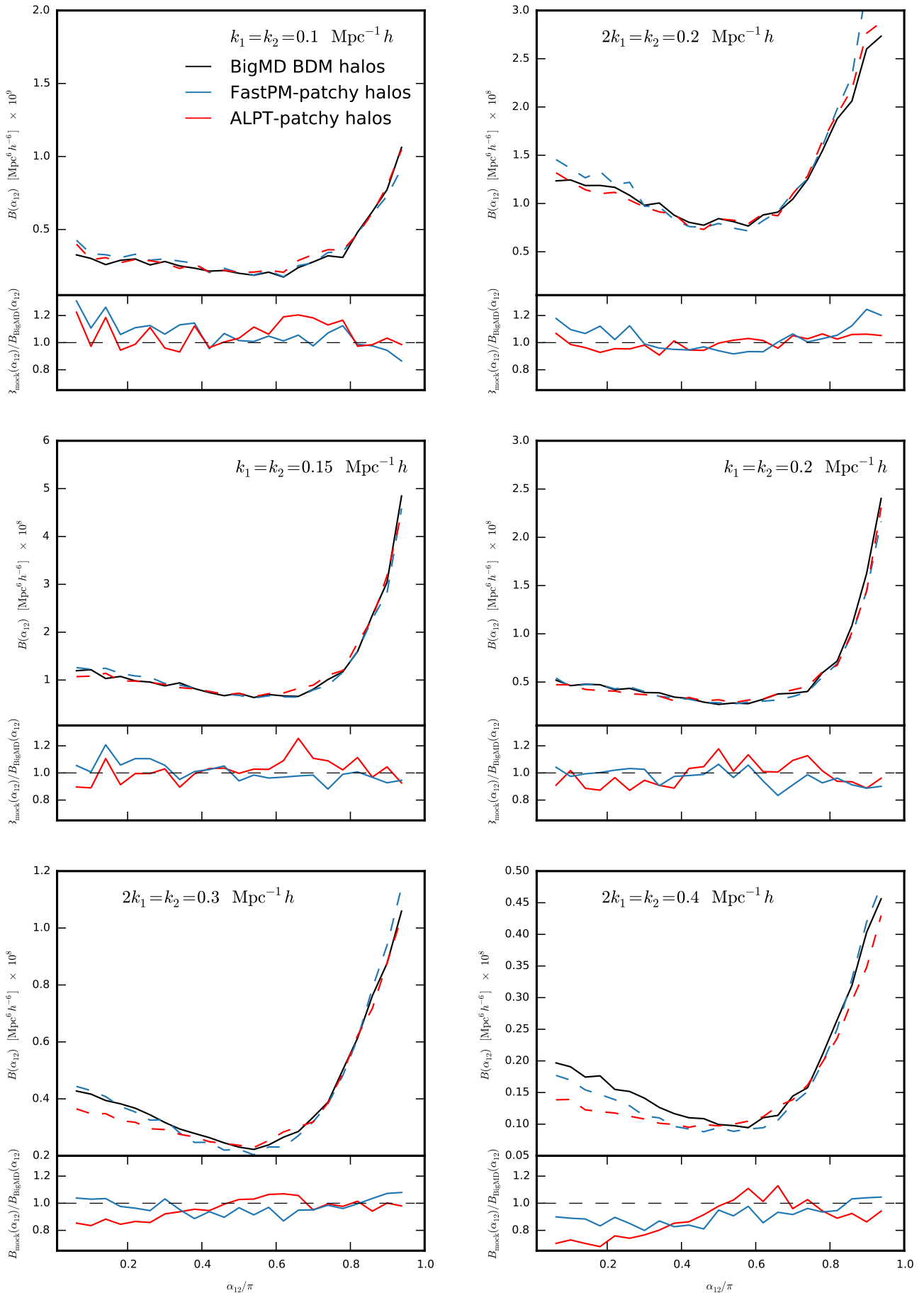


**Figure 4.** Real-space bispectrum of the BigMD BDM halos and that of the approximate mocks as a function of angle  $\alpha_{12}$  between  $\mathbf{k}_1$  and  $\mathbf{k}_2$  for  $k_1 = k_2 = 0.1 \text{ h Mpc}^{-1}$  (upper left),  $2k_1 = k_2 = 0.2 \text{ h Mpc}^{-1}$  (upper right),  $k_1 = k_2 = 0.15 \text{ h Mpc}^{-1}$  (middle left),  $k_1 = k_2 = 0.2 \text{ h Mpc}^{-1}$  (middle right),  $2k_1 = k_2 = 0.3 \text{ h Mpc}^{-1}$  (lower left), and  $2k_1 = k_2 = 0.4 \text{ h Mpc}^{-1}$  (lower right). The BigMD is represented by the solid black line, while ALPT-PATCHY is represented by the dashed red line, and FASTPM-PATCHY is represented by the dashed blue line.

### 4.3 Statistical comparison

In this section we discuss the statistical comparisons between the BDM halo catalog of the BigMultiDark simulation and the halo catalog generated from our method. In particular, the FASTPM-PATCHY mock is generated using the best-fit bias parameters (see Fig. 2). For the ALPT-PATCHY mocks we rely on the parameters found from previous PATCHY studies (Kitaura et al. 2016). The halo statistical summaries presented in this work are the number density, the bivariate halo probability distribution function (halo counts-in-cells), the real-space power spectrum and the real-space bispectrum.

By construction our method reproduces the exact number density of halos in the reference catalog (Eq. 4). We observe that the bivariate PDF (or halo counts-in-cells) of the reference catalog can be reproduced with good accuracy (Fig. 3).

In terms of the agreement between halo PDF of approximate mock catalog and that of the BigMultiDark simulation, we find that significant improvement can be achieved when halos are sampled from the FASTPM dark matter density field.

Furthermore, we present our comparison in terms of the power spectrum  $P$  and the bispectrum  $B$  which are the two-point function and the three-point function in Fourier space. Given the Fourier transform of the halo density field  $\delta_h(\mathbf{k})$ , the power spectrum and the bispectrum are defined as follows

$$\langle \delta_h(\mathbf{k}_1)\delta_h(\mathbf{k}_2) \rangle = (2\pi)^3 P(k_1)\delta^D(\mathbf{k}_1 + \mathbf{k}_2), \quad (10)$$

$$\langle \delta_h(\mathbf{k}_1)\delta_h(\mathbf{k}_2)\delta_h(\mathbf{k}_3) \rangle = (2\pi)^3 B(\mathbf{k}_1, \mathbf{k}_2)\delta^D(\mathbf{k}_1 + \mathbf{k}_2 + \mathbf{k}_3), \quad (11)$$

where  $\delta^D$  is the Dirac delta function. The shot-noise contribution to the power spectrum and bispectrum is modeled in the following way:

$$P_{\text{sn}}(k) = \frac{1}{\bar{n}}, \quad (12)$$

$$B_{\text{sn}}(\mathbf{k}_1, \mathbf{k}_2) = \frac{1}{\bar{n}}[P(k_1) + P(k_2) + P(k_3)] + \frac{1}{\bar{n}^2}, \quad (13)$$

where  $\bar{n}$  is the halo number density and  $k_3 = |\mathbf{k}_1 + \mathbf{k}_2|$ .

Our methodology is able to reproduce the halo power spectrum of the reference with  $\sim 2.5\%$  accuracy to  $k \sim 0.4 \text{ h Mpc}^{-1}$  (within 5% up to  $k \sim 0.6 \text{ h Mpc}^{-1}$ ) which corresponds to nonlinear regimes (Fig. 3). We have also run our method ignoring the PDF in the posterior sampling, yielding accurate power spectra up to  $k \sim 1 \text{ h Mpc}^{-1}$ . Kitaura et al. (2014) also reported accurate power spectra up to high  $k$ , however, using an arbitrary threshold bias of zero. In a later work additionally fitting the PDF, it was found that the power spectra are accurate within 2% up to  $k \sim 0.3 \text{ h Mpc}^{-1}$  (Kitaura et al. 2015), in agreement with what is found here using ALPT. An even higher accuracy will require a more complex bias model and a proper modeling of the clustering on sub-Mpc scales, differentiating between centrals and satellites. The current version of PATCHY randomly assigns dark matter particle positions to halos sampled in a given cell. The bias model could be augmented with non-local bias terms following McDonald & Roy (2009). We have neglected in this study the perturbation bias term used in Kitaura et al. (2016) (in an attempt to compensate for the missing power towards small scales), where the limit in the  $\sim 2\%$  level accuracy was found to be around  $k \sim 0.3 \text{ h Mpc}^{-1}$ . Omitting the perturbation theory term also allows for a fair comparison with the study

presented in Kitaura et al. (2015) and is not necessary when using FASTPM.

Fig. 3 showed an improved PDF when relying on FASTPM. This is expected to have an impact in the three point statistics, which in fact yields better fits towards small scales, as we discuss below. We show our results in terms of bispectrum for six different values of  $|\mathbf{k}_1|$  and  $|\mathbf{k}_2|$  as a function of the angle between the two vectors  $\alpha_{12} = \angle(\mathbf{k}_1, \mathbf{k}_2)$ . The adopted wave numbers are  $k_1 = k_2 = 0.1$ ,  $2k_1 = k_2 = 0.2$ ,  $k_1 = k_2 = 0.15$ ,  $k_1 = k_2 = 0.2$ ,  $2k_1 = k_2 = 0.3$ ,  $2k_1 = k_2 = 0.4$  (all wave numbers are expressed in units of  $\text{h Mpc}^{-1}$ ).

We find that in general for both ALPT and FASTPM there is good agreement between the bispectrum measured from our approximate mock catalogs and that of the BigMultiDark simulation (Fig. 4). Deviations as large as 15-20% are expected, as we are using a down-sampled white noise of the BigMultiDark simulation from  $3840^3$  to  $960^3$  cells and are on the level of what was found in Kitaura et al. (2015).

For configurations corresponding to smaller scales ( $2k_1 = k_2 = 0.3 \text{ h Mpc}^{-1}$ ,  $2k_1 = k_2 = 0.4 \text{ h Mpc}^{-1}$ ), the agreement between the bispectra of our approximate mock halo catalogs and the BigMultiDark halos improves when we sample halos from the FASTPM density field. This improvement is dramatic when compared to EZMOCKS (see real-space lines in the lower panels in Fig. 5 of Chuang et al. 2015a).

Chuang et al. (2015b) presents a comparison between the performances of different models (including ALPT-PATCHY, COLA, EZMOCKS, HALOGEN, PINOCCHIO, and PTHALOS) at recovering the distribution of BDM halos in the BigMultiDark simulation. In this comparison project one can see that ALPT-PATCHY, EZMOCKS, and COLA yield the most accurate results as compared to the reference simulation in terms of the two and three point statistics (including the quadrupole). Moreover, ALPT-PATCHY and EZMOCKS were shown to be the less computationally demanding codes using far less dark matter particles than other methods by a factor of 2.37 with respect to HALOGEN and PTHALOS, by a factor of 8 wrt PINOCCHIO, and by a factor of 64 wrt to the original N-body simulation.

## 5 SUMMARY AND DISCUSSION

This work presents a move forward towards fast and accurate generation of mock halo/galaxy catalogs, extending in particular, the PATCHY code. We have introduced an efficient MCMC technique to automatically obtain the bias parameters relating the halo/galaxy population to the underlying large scale dark matter field based on a reference catalog.

This technique is flexible and admits incorporation of different bias models, and number of bias parameters. This permits us to robustly assess the degeneracies and confidence regions of the different bias parameters.

Furthermore we have introduced in the PATCHY code a particle mesh structure formation model (the FASTPM code, see Feng et al. 2016) in addition to the previous LPT based schemes.

As a demonstration of the performance of this method, we used the halo catalog of the BigMultiDark  $N$ -body simulation as a reference catalog. Our calibration method makes use of the halo two-point statistics and the counts-in-cells to estimate the bias parameters.

Based on the dark matter field obtained with FASTPM, which includes an improved description towards small scales, and in particular, the enhanced power caused by the one halo term, we have found that previous studies based on generation of the density field with ALPT were overestimating the contribution to the power due to deviation from Poissonity. The density field generated by ALPT has missing power towards the one-halo term regime, which was partially compensated with the deterministic nonlinear bias and partially with higher stochasticity (larger deviation from Poissonity). Though present, this deviation turns out to be less pronounced when the particle mesh gravity solver is used. Also, we have managed to extend the 2.5% level accuracy of the power spectra from  $k \sim 0.3 \text{ hMpc}^{-1}$  to  $k \sim 0.6 \text{ hMpc}^{-1}$ , being at the level of percentage accuracy up to  $k \sim 0.4 \text{ hMpc}^{-1}$ .

We have demonstrated that the novel implementation of the PATCHY code reaches higher accuracy in terms of the bispectrum towards small scales with respect to LPT based schemes, such as ALPT, and even more so with respect to EZMOCKS, which relies on the Zeldovich approximation.

The assignment of halo masses must be done in a post-processing step taking into account the underlying dark matter density field. Zhao et al. (2015) demonstrated that the mass assignment is more precise when the underlying dark matter field is more accurate (ALPT vs Zeldovich). We therefore expect that using FASTPM contributes to further reduce the scatter. We leave the investigation of mass assignment for a later work. Analysis of Redshift Space Distortions will also be presented in a future work.

As we have now implemented a PM solver into our approach, we expect that certain high mass range of halos are correctly described and could be found with a friends-of-friends algorithm, the halos which are not properly resolved could be augmented with the method presented here (see methods to extend the resolution of  $N$ -body simulations, de la Torre & Peacock 2013; Angulo et al. 2015; Ahn et al. 2015).

It is important to note that our investigation in this work has been focused on the generation of high mass halo (and subhalo) catalogs. One of the main challenges toward generation of mock galaxy catalogs is sampling of low mass halos. These host fainter galaxies which will dominate the observed galaxy samples in upcoming galaxy survey datasets.

We leave a thorough investigation of the production of low mass halo catalogs to a future work. This will presumably require more sophisticated bias models including also nonlocal bias terms. The robust, automatic, and efficient methodology presented in this work should be capable of dealing with this.

In summary, the work presented here contributes to set the basis for a method able to generate galaxy mock catalogs needed to meet the precision requirements of the next generation of galaxy surveys.

## ACKNOWLEDGMENTS

We are grateful to David W. Hogg, Jeremy L. Tinker, Michael R. Blanton, Uros Seljak, Roman Scoccimarro, and Alex I. Malz for discussions related to this work. MV is particularly thankful to David W. Hogg for his

continuous support during the completion of this work. FSK thanks Uros Seljak for hospitality at UC Berkeley and LBNL during January to July 2016. During this time he met MV and was able to collaborate with YF. This work was supported by the NSF grant AST-1517237. GY acknowledges financial support from MINECO/FEDER (Spain) under research grant AYA2015-63810-P. Most of the computations in this work were carried out in the New York University High Performance Computing Merger facility. We thank Shenglong Wang, the administrator of the NYU HPC center, for his consistent support throughout the completion of this study.

The CosmoSim database used in this paper is a service by the Leibniz-Institute for Astrophysics Potsdam (AIP). The MultiDark database was developed in cooperation with the Spanish MultiDark Consolider Project CSD2009-00064. The authors gratefully acknowledge the Gauss Centre for Supercomputing e.V. (www.gauss-centre.eu) and the Partnership for Advanced Supercomputing in Europe (PRACE, www.prace-ri.eu) for funding the MultiDark simulation project by providing computing time on the GCS Supercomputer SuperMUC at Leibniz Supercomputing Centre (LRZ, www.lrz.de).

## References

- Ahn, K., Iliev, I. T., Shapiro, P. R., Srisawat, C. 2015, MNRAS, 450, 1486
- Angulo, R. E., Baugh, C. M., Frenk, C. S., Lacey, C. G. 2014, MNRAS, 442, 3256
- Ata, M., Kitaura, F.-S., Müller, V. 2015, MNRAS, 446, 4250
- Avila, S., Murray, S. G., Knebe, A., et al. 2015, MNRAS, 450, 1856
- Bagla, J. S. 2002, Journal of Astrophysics and Astronomy, 23, 185
- Bardeen, J. M., Bond, J. R., Kaiser, N., & Szalay, A. S. 1986, ApJ, 304, 15
- Blot, L., Corasaniti, P. S., Amendola, L., & Kitching, T. D. 2016, MNRAS, 458, 4462
- Bouchet, F. R., Colombi, S., Hivon, E., & Juszkiewicz, R. 1995, A&A, 296, 575
- Buchert, T., & Ehlers, J. 1993, MNRAS, 264,
- Catelan, P. 1995, MNRAS, 276, 115
- Casas-Miranda, R., Mo, H. J., Sheth, R. K., & Boerner, G. 2002, MNRAS, 333, 730
- Cen, R., & Ostriker, J. P. 1993, ApJ, 417, 415
- Chuang, C.-H., Kitaura, F.-S., Prada, F., Zhao, C., & Yepes, G. 2015, MNRAS, 446, 2621
- Chuang, C.-H., Zhao, C., Prada, F., et al. 2015, MNRAS, 452, 686
- Crocce, M., Cabré, A., & Gaztañaga, E. 2011, MNRAS, 414, 329
- Davis, M., Efstathiou, G., Frenk, C. S., & White, S. D. M. 1985, ApJ, 292, 371
- Dawson, K. S., Schlegel, D. J., Ahn, C. P., et al. 2013, AJ, 145, 10
- Dawson, K. S., Kneib, J.-P., Percival, W. J., et al. 2016, AJ, 151, 44
- de la Torre, S., & Peacock, J. A. 2013, MNRAS, 435, 743
- Dodelson, S., & Schneider, M. D. 2013, Phys. Rev. D, 88, 063537
- Feldman, H. A., Kaiser, N., & Peacock, J. A. 1994, ApJ, 426, 23

- Feng, Y., Chu, M.-Y., Seljak, U., & McDonald, P. 2016, *MNRAS*, 463, 2273
- Foreman-Mackey, D., Hogg, D. W., Lang, D., & Goodman, J. 2013, *PASP*, 125, 306
- Foreman-Mackey, D. 2016, *The Journal of Open Source Software*, 24, [Url = http://dx.doi.org/10.5281/zenodo.45906](http://dx.doi.org/10.5281/zenodo.45906)
- Frieman, J., & Dark Energy Survey Collaboration 2013, *American Astronomical Society Meeting Abstracts #221*, 221, 335.01
- Fry, J. N., & Gaztanaga, E. 1993, *ApJ*, 413, 447
- Gelman, A., & Rubin, D. B. 1992, *Statistical Science*, 457
- Gil-Marín, H., Percival, W. J., Verde, L., et al. 2017, *MNRAS*, 465, 1757
- Gil-Marín, H., Noreña, J., Verde, L., et al. 2015, *MNRAS*, 451, 539
- Gil-Marín, H., Verde, L., Noreña, J., et al. 2015, *MNRAS*, 452, 1914
- Goodman, J., & Weare, J. 2010, *Communications in applied mathematics and computational science*, 5, 65
- Grieb, J. N., Sánchez, A. G., Salazar-Albornoz, S., & Dalla Vecchia, C. 2016, *MNRAS*, 457, 1577
- Guo, H., Zheng, Z., Behroozi, P. S., et al. 2016, *ApJ*, 831, 3
- Hartlap, J., Simon, P., & Schneider, P. 2007, *A&A*, 464, 399
- Howlett, C., Manera, M., & Percival, W. J. 2015, *Astronomy and Computing*, 12, 109
- Izard, A., Crocce, M., & Fosalba, P. 2016, *MNRAS*, 459, 2327
- Joachimi, B. 2016, [arXiv:1612.00752](https://arxiv.org/abs/1612.00752)
- Kaiser, N. 1984, *ApJ*, 284, L9
- Kitaura, F.-S., & Heß, S. 2013, *MNRAS*, 435, L78
- Kitaura, F.-S., Yepes, G., & Prada, F. 2014, *MNRAS*, 439, L21
- Kitaura, F.-S., Gil-Marín, H., Scóccola, C. G., et al. 2015, *MNRAS*, 450, 1836
- Kitaura, F.-S., Rodríguez-Torres, S., Chuang, C.-H., et al. 2016, *MNRAS*, 456, 4156
- Kalus, B., Percival, W. J., & Samushia, L. 2016, *MNRAS*, 455, 2573
- Klypin, A., & Holtzman, J. 1997, [arXiv:astro-ph/9712217](https://arxiv.org/abs/astro-ph/9712217)
- Klypin, A., Yepes, G., Gottlöber, S., Prada, F., & Heß, S. 2016, *MNRAS*, 457, 4340
- Knebe, A., Knollmann, S. R., Muldrew, S. I., et al. 2011, *MNRAS*, 415, 2293
- Koda, J., Blake, C., Beutler, F., Kazin, E., & Marin, F. 2016, *MNRAS*, 459, 2118
- Laureijs, R., Amiaux, J., Arduini, S., et al. 2011, [arXiv:1110.3193](https://arxiv.org/abs/1110.3193)
- Ledoit, O., & Wolf, M. 2004, *Journal of Multivariate Analysis*, 88, 365
- Ledoit, O., & Wolf, M. 2012, *The Annals of Statistics*, 40, 1024
- Levi, M., Bebek, C., Beers, T., et al. 2013, [arXiv:1308.0847](https://arxiv.org/abs/1308.0847)
- LSST Science Collaboration, Abell, P. A., Allison, J., et al. 2009, [arXiv:0912.0201](https://arxiv.org/abs/0912.0201)
- Manera, M., Scoccimarro, R., Percival, W. J., et al. 2013, *MNRAS*, 428, 1036
- Manera, M., Samushia, L., Tojeiro, R., et al. 2015, *MNRAS*, 447, 437
- McDonald, P., Roy, A. 2009, *J. Cosmology Astropart. Phys.*, 8, 20
- Mo, H. J., & White, S. D. M. 2002, *MNRAS*, 336, 112
- Monaco, P., Theuns, T., Taffoni, G. et al. 2002, *ApJ*, 564, 8
- Monaco, P., Sefusatti, E., Borgani, S., et al. 2013, *MNRAS*, 433, 2389
- Monaco, P. 2016, *Galaxies*, 4, 53
- Morrison, C. B., & Schneider, M. D. 2013, *J. Cosmology Astropart. Phys.*, 11, 009
- Navarro, J. F., Frenk, C. S., & White, S. D. M. 1996, *ApJ*, 462, 563
- Neyrinck, M. C., Aragón-Calvo, M. A., Jeong, D., & Wang, X. 2014, *MNRAS*, 441, 646
- Padmanabhan, N., White, M., Zhou, H. H., & O'Connell, R. 2016, *MNRAS*, 460, 1567
- Peebles, P. J. E. 1980, *Research supported by the National Science Foundation*. Princeton, N.J., Princeton University Press, 1980. 435 p.,
- Pope, A. C., & Szapudi, I. 2008, *MNRAS*, 389, 766
- Rodríguez-Torres, S. A., Chuang, C.-H., Prada, F., et al. 2016, *MNRAS*, 460, 1173
- Schneider, P., van Waerbeke, L., Kilbinger, M., & Mellier, Y. 2002, *A&A*, 396, 1
- Scoccimarro, R., Sheth, R. K. 2002, *MNRAS*, 329, 629
- Sheth, R. K., Mo, H. J., & Tormen, G. 2001, *MNRAS*, 323, 1
- Simpson, F., Blake, C., Peacock, J. A., et al. 2016, *Phys. Rev. D*, 93, 023525
- Slepian, Z., Eisenstein, D. J., Beutler, F., et al. 2015, [arXiv:1512.02231](https://arxiv.org/abs/1512.02231)
- Slepian, Z., Eisenstein, D. J., Blazek, J. A., et al. 2016, [arXiv:1607.06098](https://arxiv.org/abs/1607.06098)
- Slepian, Z., Eisenstein, D. J., Brownstein, J. R., et al. 2016, [arXiv:1607.06097](https://arxiv.org/abs/1607.06097)
- Smith, R. E., Scoccimarro, R., & Sheth, R. K. 2008, *Phys. Rev. D*, 77, 043525
- Somerville, R. S., Lemson, G., Sigad, Y., et al. 2001, *MNRAS*, 320, 289
- Spergel, D., Gehrels, N., Baltay, C., et al. 2015, [arXiv:1503.03757](https://arxiv.org/abs/1503.03757)
- Springel, V. 2005, *MNRAS*, 364, 1105
- Sun, L., Wang, Q., & Zhan, H. 2013, *ApJ*, 777, 75
- Tassev, S., Zaldarriaga, M., & Eisenstein, D. J. 2013, *J. Cosmology Astropart. Phys.*, 6, 036
- Tassev, S., Eisenstein, D. J., Wandelt, B. D., & Zaldarriaga, M. 2015, [arXiv:1502.07751](https://arxiv.org/abs/1502.07751)
- Taylor, A., Joachimi, B., & Kitching, T. 2013, *MNRAS*, 432, 1928
- Taylor, A., & Joachimi, B. 2014, *MNRAS*, 442, 2728
- White, M., Blanton, M., Bolton, A., et al. 2011, *ApJ*, 728, 126
- White, M., Tinker, J. L., & McBride, C. K. 2014, *MNRAS*, 437, 2594
- Zhao, C., Kitaura, F.-S., Chuang, C.-H., et al. 2015, *MNRAS*, 451, 4266